INTERNATIONAL JOURNAL FOR NUMERICAL METHODS IN FLUIDS
Int. J. Numer. Meth. Fluids 2007; **53**:471–484
Published online 6 July 2006 in Wiley InterScience (www.interscience.wiley.com). DOI: 10.1002/fld.1290

A robust numerical method for flow through a pipe driven by an oscillating pressure gradient

Ali R. Ansari[1,*,†], John J. H. Miller[2,3,‡] and Grigori I. Shishkin[4,§]

[1]*Department of Mathematics and Physical Sciences, Gulf University for Science and Technology, P.O. Box 7207, Hawally 32093, Kuwait*
[2]*Department of Mathematics, Trinity College, Dublin 2, Ireland*
[3]*Department of Computational Science, National University of Singapore, Singapore 11754, Singapore*
[4]*Institute of Mathematics and Mechanics, Russian Academy of Sciences, Ural Branch, Ekaterinberg, Russia*

SUMMARY

The problem of periodic flow of an incompressible fluid through a pipe, which is driven by an oscillating pressure gradient (e.g. a reciprocating piston), is investigated in the case of a large Reynolds number. This process is described by a singularly perturbed parabolic equation with a periodic right-hand side, where the singular perturbation parameter is the viscosity v. The periodic solution of this problem is a solution of the Navier–Stokes equations with cylindrical symmetry. We are interested in constructing a parameter-robust numerical method for this problem, i.e. a numerical method generating numerical approximations that converge uniformly with respect to the parameter v and require a bounded time, independent of the value of v, for their computation. Our method comprises a standard monotone discretization of the problem on non-standard *piecewise uniform* meshes condensing in a neighbourhood of the boundary layer. The transition point between segments of the mesh with different step sizes is chosen in accordance with the behaviour of the analytic solution in the boundary layer region. In this paper we construct the numerical method and discuss the results of extensive numerical experiments, which show experimentally that the method is parameter-robust. Copyright © 2006 John Wiley & Sons, Ltd.

Received 6 October 2003; Revised 26 December 2005; Accepted 28 April 2006

KEY WORDS: oscillating pressure gradient; piecewise-uniform mesh; parameter-robust approximations; pipe flow

*Correspondence to: A. R. Ansari, Department of Mathematics and Physical Sciences, Gulf University for Science and Technology, P.O. Box 7207, Hawally 32093, Kuwait.
†E-mail: ansari.a@gust.edu.kw
‡E-mail: jmiller@tcd.ie, http://www.maths.tcd.ie/∼miller
§E-mail: shishkin@imm.uran.ru, http://www.home.imm.uran.ru/SPP

Contract/grant sponsor: Enterprise Ireland Research Grant; contract/grant number: SC-2000-070
Contract/grant sponsor: Russian Foundation for Basic Research; contract/grant number: 04-01-00578
Contract/grant sponsor: University of Limerick

Copyright © 2006 John Wiley & Sons, Ltd.

1. INTRODUCTION

The recent development of novel piecewise uniform fitted mesh techniques [1] has facilitated considerable advancement in the numerical solution of singularly perturbed differential equations. Linear problems of this type have been solved with these techniques yielding numerical solutions that exhibit convergence uniformly with respect to the singular perturbation parameter, while the computational work required to obtain these solutions is also independent of this parameter [2–4]; we refer to numerical methods with this property as parameter-robust methods. These fitted mesh techniques have also been applied successfully to the computation of parameter-robust solutions of non-linear problems [4–7]. Ultimately we are interested in the development of parameter-robust numerical methods for solving the Navier–Stokes equations. To realize this goal, we need to gain more insight into techniques for overcoming the many obstacles that lie in the path. For this reason it is useful to construct numerical methods for the solution of simpler problems with known solutions. Thus far, flow problems with only a zero pressure gradient have been considered. Furthermore, all of these problems have steady boundary layers [8]. Our objective here is to consider more complicated problems, in which not only is the boundary layer unsteady [8, 9], but also the flow is driven by a periodic pressure gradient. One problem with these attributes is flow in a pipe under the influence of a reciprocating piston [8].

We denote the co-ordinate along the axis of the pipe by x and the radial distance by r. We assume that the pipe has a constant circular cross section with radius R. We further assume that the pipe is long, so that the flow can be taken to be independent of x. This means that the axial velocity component is independent of x, and thus the other velocity components vanish along with the convective terms that are parallel to the pipe. Therefore, the full Navier–Stokes equations in cylindrical co-ordinates for this problem [8] reduce to

$$\frac{\partial u}{\partial t} = -\frac{1}{\rho}\frac{\partial p}{\partial x} + \nu\left(\frac{\partial^2 u}{\partial r^2} + \frac{1}{r}\frac{\partial u}{\partial r}\right) \tag{1}$$

where u is the axial velocity, p is the pressure, ρ is the density and ν is the viscosity of the fluid. The boundary condition on the wall of the pipe is the usual no-slip condition

$$u(t, R) = 0 \tag{2}$$

i.e. the velocity is zero at the wall. This determines the location of the boundary layer. Assuming that the oscillations of the pressure gradient are harmonic with period $T = 2\pi/n$ we have

$$-\frac{1}{\rho}\frac{\partial p}{\partial x} = \gamma \cos nt \tag{3}$$

where γ denotes a constant and n is the frequency of the oscillations. Here R and $T = 2\pi/n$ are constants independent of the singular perturbation parameter ν.

Problems (1)–(3) are a periodic problem on the rectangle $\overline{\Omega}$, where

$$\overline{\Omega} = \Omega \cup \Gamma, \quad \Omega = (0, R) \times (0, T) \tag{4}$$

The boundary of Ω is $\Gamma = \Gamma_L \cup \Gamma_R \cup \Gamma_T \cup \Gamma_0$ where $\Gamma_L, \Gamma_R, \Gamma_T$ and Γ_0 denote the left, right, top and bottom edges of Ω, respectively. We seek the solution of Equations (1)–(3) on Ω subject

Copyright © 2006 John Wiley & Sons, Ltd.

DOI: 10.1002/fld

to the additional boundary conditions

$$u|_{\Gamma_0} = u|_{\Gamma_T} \tag{5}$$

$$\frac{\partial}{\partial r} u|_{\Gamma_L} = 0 \tag{6}$$

Note that the boundary condition (5) ensures that the solution is periodic in time, while the boundary condition (6) reflects the symmetry of the problem.

Problems (1)–(6) has the exact periodic solution [8]

$$u(r, t) = -\mathrm{i}\frac{\gamma}{n} e^{\mathrm{i}nt}\left[1 - \frac{J_o\left(r\sqrt{\frac{-\mathrm{i}n}{\nu}}\right)}{J_o\left(R\sqrt{\frac{-\mathrm{i}n}{\nu}}\right)}\right] \tag{7}$$

where J_o is the Bessel function of the first kind of order zero and $\mathrm{i} = \sqrt{-1}$. Furthermore, some simple analysis [8, 10] shows that the thickness of the boundary layer ξ is

$$\xi \sim \sqrt{\frac{\nu}{n}} \tag{8}$$

Typically, such flow problems exhibit a two zone structure, namely, the inviscid core flow and the layer flow close to the wall. For our analysis we assume that n is fixed. Note that the layer arises when the value ν/n is small (that is, when ν is small and/or n is large).

Since the second derivative term in the equation of motion (1) is multiplied by the viscosity ν, where ν may be arbitrarily small, this equation is clearly a singularly perturbed differential equation with ν as the singular perturbation parameter. In the case of steady boundary layers, the layer thickness depends only on the singular perturbation parameter. Here, however, the situation is different: the boundary layer is unsteady and so account must be taken of the time spent by a fluid particle in the layer, which depends on the frequency of the harmonic oscillation. We will consider this in more detail later.

Our objective is to obtain numerical solutions to this periodic problem, that are robust with respect to ν for a fixed frequency $n = 1$. The sensitivity of classical numerical methods to the singular perturbation parameter is reflected by the fact that the maximum pointwise errors, in the numerical approximations produced by such methods, become unacceptably large for small ν. This has been shown for linear problems, e.g. in Reference [2], and more recently for non-linear problems in Reference [5], where it is also shown that this difficulty is not resolved unless the meshes are appropriately fitted to the boundary layer. The numerical method constructed here comprises appropriately fitted piecewise-uniform meshes [4, 5, 11, 12] in conjunction with an upwind finite difference operator [4, 12]. This is a *parameter-robust* numerical method for problems (1)–(6), as is shown experimentally in the following sections by extensive numerical computations.

As mentioned earlier, the full Navier–Stokes equations in cylindrical co-ordinates reduce to (1) for this problem. But there is no known *parameter-robust* method for solving the Navier–Stokes equations, even for this simple geometry, so it is worthwhile considering the numerical solution of this simple model problem, even for those values of ν for which this formulation is not physically

Copyright © 2006 John Wiley & Sons, Ltd.

DOI: 10.1002/fld

valid. Note that, even though the values of v may become physically invalid, when they are taken in conjunction with the frequency n, they may still be acceptable.

2. A ROBUST FINITE DIFFERENCE SCHEME

We want to construct a v-robust finite difference method for problems (1)–(6). We first define the fitted piecewise uniform mesh for this method. On the finite rectangular domain $\overline{\Omega}$, corresponding to a single period of the pressure gradient oscillation, we place a rectangular mesh $\overline{\Omega}_v^{\mathbf{N}}$, which is the tensor product

$$\overline{\Omega}_v^{\mathbf{N}} = \overline{\Omega}_v^{N_r} \times \overline{\Omega}^{N_t} \tag{9}$$

where $\mathbf{N} = (N_r, N_t)$. Here $\overline{\Omega}^{N_t}$ is a uniform mesh on the interval $[0, T]$ with N_t mesh intervals, while $\overline{\Omega}_v^{N_r}$ is a piecewise uniform fitted mesh on the interval $[0, R]$ with N_r mesh intervals. To fit the piecewise uniform mesh $\overline{\Omega}_v^{N_r}$ to the boundary layer, the interval $[0, R]$ is divided into two subintervals $[0, R-\sigma]$ and $[R-\sigma, R]$, $\sigma \leqslant R/2$. Then $N_r/2$ equidistant mesh intervals are assigned to each subinterval. Here we take $N_r = N_t = N$ and so

$$r_i = \begin{cases} 2i(1-\sigma)/N, & i = 0, 1, 2, \ldots N/2 \\ R - \sigma + 2(i - N/2)(1 - (R-\sigma))/N, & i = N/2, \ldots, N \end{cases} \tag{10}$$

with $t_j = t_{j-1} + h$, $j = 1, \ldots, N$, $h = 2\pi/N$.

The correct choice of the transition point σ is of particular significance, since, by reducing σ as v decreases, the mesh condenses in the σ-neighbourhood of the set $r = R$. Following the principles set out in References [3, 4], the value of σ is chosen to be

$$\sigma = \min \left\{ \tfrac{1}{2}R, C v^{1/2} \ln N \right\}$$

where C is an arbitrary constant. The factor $v^{1/2}$ is motivated from (8), while experimentation suggests that $C = \sqrt{2}$ is a reasonable value.

Using this fitted piecewise uniform mesh, the upwind operator for the discretization of (1) and a standard discretization of the boundary conditions (2), (5) and (6), we obtain on $\Omega_v^{\mathbf{N}}$ the monotone finite difference method

$$-v\left[\delta_r^2 U_v(r_i, t_j) + \frac{1}{r_i} D_r^+ U_v(r_i, t_j)\right] + D_t^- U_v(r_i, t_j) - \gamma \cos n t_j = 0 \tag{11}$$

$$\begin{aligned} U_v(R, t_j) = 0 \quad \text{all } t_j \in \Gamma_R, \quad U_v(r_i, 0) = U_v(r_i, T) \quad \text{all } r_i \in \Gamma_0 \\ D_r^+ U_v(0, t_j) = 0 \quad \text{all } t_j \in \Gamma_L \end{aligned} \tag{12}$$

where

$$D_r^+ U_v(r_i, t_j) \equiv \frac{U_v(r_{i+1}, t_j) - U_v(r_i, t_j)}{r_{i+1} - r_i}, \quad D_r^- U_v(r_i, t_j) \equiv \frac{U_v(r_i, t_j) - U_v(r_{i-1}, t_j)}{r_i - r_{i-1}}$$

Copyright © 2006 John Wiley & Sons, Ltd.

DOI: 10.1002/fld

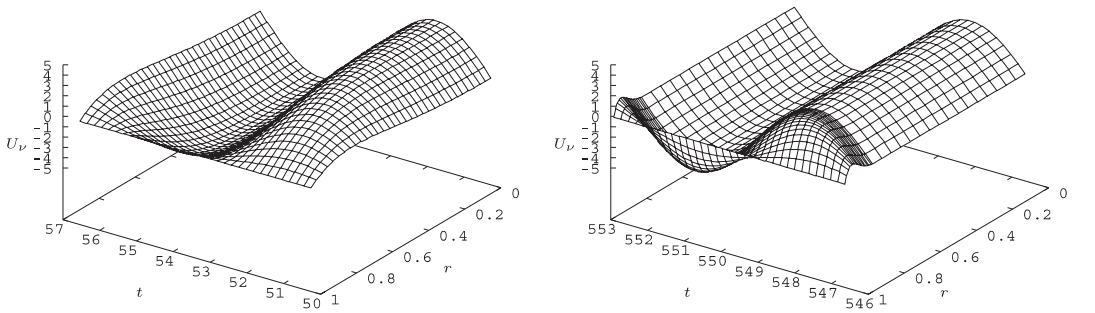

Figure 1. Surface plot of numerical solutions for $v = 2^{-5}$ and $v = 2^{-10}$ on a fitted piecewise uniform mesh with $N = 32$ and $\text{tol} = 10^{-3}$.

with an analogous definition of $D_t^- U_v(r_i, t_j)$, and

$$\delta_r^2 U_v(r_i, t_j) \equiv \frac{D_r^+ U_v(r_i, t_j) - D_r^- U_v(r_i, t_j)}{(r_{i+1} - r_{i-1})/2}$$

We solve the discrete problem (11), (12) using the following iterative process. We take an initial guess

$$U(r_i, 0) = u_0(r_i) \tag{13}$$

for all $r_i \in \Gamma_0$, where u_0 is an arbitrary function (we take $u_0 = 0$). We solve the discrete problem for the function $U_v(r_i, t_j)$, for $j = 1, 2, \ldots, N$, satisfying Equation (11) and the boundary conditions (12) by a marching algorithm. We take $U(r_i, T)$ to be the new values for $u_0(r_i)$, $i = 1, 2, \ldots, N$ in (13) and repeat the marching algorithm. This process is repeated until we reach a numerical solution that is periodic up to a prescribed tolerance tol, in the sense that

$$\max_{0 \leqslant i \leqslant N} |U_v(r_i, T) - U_v(r_i, 0)|_{\overline{\Omega}_v^{\mathbf{N}}} \leqslant \text{tol} \tag{14}$$

Our main purpose in what follows is to show experimentally that the numerical solutions of the finite difference scheme (11), (12), satisfying (14), converges v-uniformly to the solution of the periodic problem.

To illustrate the boundary layer behaviour we plot the solution of problem (11), (12) for $v = 2^{-5}$ and $v = 2^{-10}$ with $N = 32$ in Figure 1. The desired tolerance (14) is achieved after 8 iterations for $v = 2^{-5}$ and 87 iterations for $v = 2^{-10}$. Note that we have used a non-standard orientation of the graph for a clearer view of the boundary layer.

Since we know the exact solution of the problem, in this case we can directly determine the error. We denote by U_v^{2048} the numerical solution on the finest mesh, which here corresponds to $N = 2048$, and by $\bar{U}_v^{2048}$ its piecewise linear interpolant. We take $\bar{U}_v^{2048}$ as the reference solution. We then introduce the computed pointwise errors with respect to the finest mesh

$$E_v^N = \|U_v^N - \bar{U}_v^{2048}\|_{\Omega_v^N} \tag{15}$$

The associated computed v-uniform pointwise errors are

$$E^N = \max_v E_v^N \tag{16}$$

Copyright © 2006 John Wiley & Sons, Ltd.

DOI: 10.1002/fld

Table I. Errors E_v^N and E^N for various values of v and N.

	Number of intervals N					
v	32	64	128	256	512	1024
2^{-1}	0.113D+00	0.575D−01	0.282D−01	0.133D−01	0.571D−02	0.191D−02
2^{-2}	0.264D+00	0.135D+00	0.664D−01	0.313D−01	0.135D−01	0.449D−02
2^{-3}	0.468D+00	0.238D+00	0.117D+00	0.551D−01	0.237D−01	0.792D−02
2^{-4}	0.587D+00	0.296D+00	0.145D+00	0.682D−01	0.293D−01	0.979D−02
2^{-5}	0.540D+00	0.269D+00	0.131D+00	0.614D−01	0.263D−01	0.878D−02
2^{-6}	0.458D+00	0.227D+00	0.110D+00	0.516D−01	0.221D−01	0.738D−02
2^{-7}	0.447D+00	0.222D+00	0.108D+00	0.506D−01	0.217D−01	0.723D−02
2^{-8}	0.439D+00	0.218D+00	0.106D+00	0.498D−01	0.214D−01	0.724D−02
2^{-9}	0.434D+00	0.216D+00	0.105D+00	0.492D−01	0.211D−01	0.716D−02
2^{-10}	0.431D+00	0.216D+00	0.106D+00	0.515D−01	0.322D−01	0.115D−01
2^{-11}	0.432D+00	0.236D+00	0.141D+00	0.862D−01	0.377D−01	0.126D−01
2^{-12}	0.488D+00	0.299D+00	0.184D+00	0.863D−01	0.370D−01	0.124D−01
2^{-13}	0.603D+00	0.378D+00	0.184D+00	0.863D−01	0.371D−01	0.124D−01
2^{-14}	0.768D+00	0.380D+00	0.184D+00	0.862D−01	0.371D−01	0.124D−01
2^{-15}	0.773D+00	0.380D+00	0.184D+00	0.862D−01	0.371D−01	0.124D−01
2^{-16}	0.773D+00	0.380D+00	0.184D+00	0.862D−01	0.371D−01	0.124D−01
2^{-17}	0.773D+00	0.380D+00	0.184D+00	0.861D−01	0.371D−01	0.124D−01
2^{-18}	0.773D+00	0.380D+00	0.184D+00	0.861D−01	0.370D−01	0.124D−01
2^{-19}	0.773D+00	0.380D+00	0.184D+00	0.861D−01	0.371D−01	0.124D−01
2^{-20}	0.773D+00	0.380D+00	0.184D+00	0.861D−01	0.370D−01	0.124D−01
E^N	0.773D+00	0.380D+00	0.184D+00	0.863D−01	0.377D−01	0.126D−01

Table II shows the errors E_v^N and E^N. We note that all of the results shown in this, and all subsequent tables, are for solutions for which criterion (14) is satisfied with $\mathrm{tol} = 10^{-3}$. We see from Table II that the entries are decreasing along each of the rows with increasing N. In addition, the entries decrease and stabilize at values around $v = 2^{-15}$ for all N. The numerical results in Table II demonstrate experimentally that the numerical solutions converge v-uniformly.

We now analyse the errors in the numerical solutions in a different way, which does not depend on *a priori* knowledge of the exact solution. We introduce the computed pointwise two-mesh differences

$$D_v^N = \|U_v^N - \bar{U}_v^{2N}\|_{\Omega_v^N} \tag{17}$$

which are the differences between the numerical solutions computed on the meshes Ω_v^N and Ω_v^{2N} (see, e.g. References [3, 4]). The associated computed v-uniform pointwise two-mesh differences are given by

$$D^N = \max_v D_v^N \tag{18}$$

Copyright © 2006 John Wiley & Sons, Ltd.

DOI: 10.1002/fld

Table II. Two mesh differences D_v^N and D^N for various values of v and N.

	Number of intervals N				
v	32	64	128	256	512
2^{-1}	0.562D−01	0.294D−01	0.150D−01	0.757D−02	0.380D−02
2^{-2}	0.130D+00	0.686D−01	0.352D−01	0.178D−01	0.896D−02
2^{-3}	0.231D+00	0.121D+00	0.620D−01	0.314D−01	0.158D−01
2^{-4}	0.292D+00	0.151D+00	0.770D−01	0.389D−01	0.195D−01
2^{-5}	0.272D+00	0.138D+00	0.698D−01	0.350D−01	0.176D−01
2^{-6}	0.232D+00	0.117D+00	0.590D−01	0.295D−01	0.148D−01
2^{-7}	0.224D+00	0.114D+00	0.575D−01	0.289D−01	0.145D−01
2^{-8}	0.220D+00	0.112D+00	0.564D−01	0.285D−01	0.143D−01
2^{-9}	0.217D+00	0.111D+00	0.558D−01	0.280D−01	0.141D−01
2^{-10}	0.216D+00	0.111D+00	0.556D−01	0.308D−01	0.206D−01
2^{-11}	0.217D+00	0.111D+00	0.578D−01	0.486D−01	0.251D−01
2^{-12}	0.221D+00	0.116D+00	0.975D−01	0.494D−01	0.246D−01
2^{-13}	0.230D+00	0.194D+00	0.982D−01	0.492D−01	0.247D−01
2^{-14}	0.387D+00	0.196D+00	0.982D−01	0.492D−01	0.247D−01
2^{-15}	0.393D+00	0.196D+00	0.982D−01	0.492D−01	0.247D−01
2^{-16}	0.393D+00	0.196D+00	0.982D−01	0.492D−01	0.247D−01
2^{-17}	0.393D+00	0.196D+00	0.982D−01	0.492D−01	0.247D−01
2^{-18}	0.393D+00	0.196D+00	0.982D−01	0.492D−01	0.246D−01
2^{-19}	0.393D+00	0.196D+00	0.982D−01	0.492D−01	0.247D−01
2^{-20}	0.393D+00	0.196D+00	0.982D−01	0.492D−01	0.246D−01
D^N	0.393D+00	0.196D+00	0.982D−01	0.494D−01	0.251D−01

We use the pointwise two-mesh differences D_v^N to define the pointwise orders of convergence

$$R_v^N = \log_2 \frac{D_v^N}{D_v^{2N}} \tag{19}$$

Furthermore, we use the v-uniform two mesh differences D^N to define the computed v-uniform orders of convergence

$$R^N = \log_2 \frac{D^N}{D^{2N}} \tag{20}$$

Following the technique in Reference [4] we introduce a final v-uniform order of convergence

$$R^* = \min_N R^N \tag{21}$$

The same technique gives us the computed v-uniform error constant

$$C_{R^*}^* = \max_N C_{R^*}^N \tag{22}$$

Copyright © 2006 John Wiley & Sons, Ltd.

DOI: 10.1002/fld

Table III. Orders of convergence R_v^N for various values of v and N.

	Number of intervals N			
v	32	64	128	256
2^{-1}	0.94	0.97	0.99	0.99
2^{-2}	0.93	0.96	0.98	0.99
2^{-3}	0.93	0.97	0.98	0.99
2^{-4}	0.95	0.97	0.99	0.99
2^{-5}	0.97	0.99	0.99	1.00
2^{-6}	0.99	0.99	1.00	1.00
2^{-7}	0.97	0.99	0.99	1.00
2^{-8}	0.97	0.99	0.99	1.00
2^{-9}	0.97	0.99	0.99	0.99
2^{-10}	0.96	0.99	0.85	0.58
2^{-11}	0.96	0.94	0.25	0.95
2^{-12}	0.93	0.24	0.98	1.00
2^{-13}	0.24	0.98	1.00	0.99
2^{-14}	0.98	1.00	1.00	0.99
2^{-15}	1.00	1.00	1.00	0.99
2^{-16}	1.00	1.00	1.00	0.99
2^{-17}	1.00	1.00	1.00	0.99
2^{-18}	1.00	1.00	1.00	1.00
2^{-19}	1.00	1.00	1.00	0.99
2^{-20}	1.00	1.00	1.00	1.00
R^N	1.00	1.00	0.99	0.98

Table IV. Computed v-uniform orders of convergence, error constants, error bounds and error for various values of N.

	Number of intervals N				
	32	64	128	256	
R^N	1.00	1.00	0.99	0.98	$(R^* = 0.98)$
$C_{0.98}^N$	23.80	23.41	23.14	22.96	$(C_{0.98}^* = 23.80)$
$C_{0.98}^* N^{-0.98}$	0.797	0.404	0.205	0.104	
E^N	0.773	0.380	0.184	0.0863	

and thus a computed upper bound for the error $C_{R^*}^* N^{-R^*}$ where the quantities $C_{R^*}^N$ are computed from

$$C_{R^*}^N = \frac{D^N N^{R^*}}{1 - 2^{-R^*}} \tag{23}$$

Values of the computed two mesh differences D_v^N and D^N are given in Table II and the corresponding computed R^N in Table III. In Tables I and II we notice that the errors are reducing

Copyright © 2006 John Wiley & Sons, Ltd.

DOI: 10.1002/fld

Table V. Number of iterations I_v^N and I^N required to satisfy (14) with $\text{tol} = 10^{-3}$ for various values of v and N.

	Number of intervals N					
v	32	64	128	256	512	1024
2^{-1}	2	2	2	2	2	2
2^{-2}	2	2	2	2	2	2
2^{-3}	3	3	3	3	3	3
2^{-4}	5	5	5	5	5	5
2^{-5}	8	8	7	7	7	7
2^{-6}	12	12	12	11	11	11
2^{-7}	20	19	18	17	17	17
2^{-8}	33	30	27	25	24	23
2^{-9}	54	47	40	34	30	27
2^{-10}	87	71	55	40	21	18
2^{-11}	134	100	62	25	19	17
2^{-12}	190	113	36	23	18	17
2^{-13}	219	63	34	22	18	16
2^{-14}	120	58	32	22	18	16
2^{-15}	110	56	32	22	18	16
2^{-16}	105	53	31	22	18	16
2^{-17}	96	53	31	21	18	16
2^{-18}	94	52	30	21	17	16
2^{-19}	55	49	31	22	18	16
2^{-20}	68	41	26	21	17	16
I^N	219	113	62	40	30	27

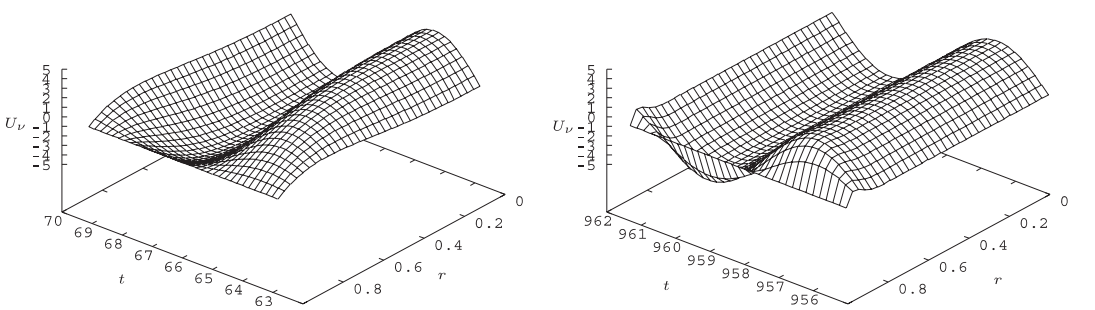

Figure 2. Surface plot of numerical solutions for $v = 2^{-5}$ and $v = 2^{-10}$ on a *uniform* mesh with $N = 32$ and $\text{tol} = 10^{-3}$.

along each of the rows for increasing N, also the errors stabilize to fixed values around $v = 2^{-15}$, except for one column, i.e. for $N = 512$ in both Tables I and II (last few rows). This is because of the choice of the tolerance and is expected. In addition, in Table III the computed R^N are computed using D^N from Table II. The numerical results in these tables demonstrate that the numerical solutions converge v-uniformly.

Copyright © 2006 John Wiley & Sons, Ltd.

DOI: 10.1002/fld

Table VI. Errors E_v^N for various values of v and N on a *uniform* mesh, with the finest mesh $N = 2048$ computed on a *uniform* mesh.

	Number of intervals N					
v	32	64	128	256	512	1024
2^{-0}	0.453D−01	0.228D−01	0.112D−01	0.525D−02	0.226D−02	0.754D−03
2^{-1}	0.113D+00	0.575D−01	0.282D−01	0.133D−01	0.571D−02	0.191D−02
2^{-2}	0.264D+00	0.135D+00	0.664D−01	0.313D−01	0.135D−01	0.449D−02
2^{-3}	0.468D+00	0.238D+00	0.117D+00	0.551D−01	0.237D−01	0.792D−02
2^{-4}	0.587D+00	0.296D+00	0.145D+00	0.682D−01	0.293D−01	0.979D−02
2^{-5}	0.540D+00	0.269D+00	0.131D+00	0.614D−01	0.263D−01	0.878D−02
2^{-6}	0.458D+00	0.227D+00	0.110D+00	0.516D−01	0.221D−01	0.738D−02
2^{-7}	0.449D+00	0.222D+00	0.108D+00	0.506D−01	0.217D−01	0.723D−02
2^{-8}	0.446D+00	0.220D+00	0.107D+00	0.499D−01	0.214D−01	0.724D−02
2^{-9}	0.447D+00	0.219D+00	0.106D+00	0.495D−01	0.212D−01	0.719D−02
2^{-10}	0.456D+00	0.223D+00	0.108D+00	0.516D−01	0.322D−01	0.115D−01
2^{-11}	0.473D+00	0.237D+00	0.142D+00	0.862D−01	0.377D−01	0.126D−01
2^{-12}	0.508D+00	0.300D+00	0.184D+00	0.863D−01	0.370D−01	0.124D−01
2^{-13}	0.609D+00	0.379D+00	0.184D+00	0.862D−01	0.371D−01	0.124D−01
2^{-14}	0.769D+00	0.380D+00	0.184D+00	0.862D−01	0.371D−01	0.124D−01
2^{-15}	0.773D+00	0.425D+00	0.184D+00	0.862D−01	0.371D−01	0.124D−01
2^{-16}	0.773D+00	0.475D+00	0.264D+00	0.862D−01	0.371D−01	0.124D−01
2^{-17}	0.773D+00	0.402D+00	0.371D+00	0.147D+00	0.375D−01	0.124D−01
2^{-18}	0.773D+00	0.380D+00	0.385D+00	0.260D+00	0.701D−01	0.141D−01
2^{-19}	0.773D+00	0.380D+00	0.293D+00	0.346D+00	0.145D+00	0.298D−01
2^{-20}	0.773D+00	0.380D+00	0.187D+00	0.335D+00	0.247D+00	0.578D−01
2^{-21}	0.773D+00	0.380D+00	0.184D+00	0.232D+00	0.315D+00	0.117D+00
2^{-22}	0.775D+00	0.380D+00	0.184D+00	0.129D+00	0.287D+00	0.192D+00
2^{-23}	0.774D+00	0.384D+00	0.184D+00	0.928D−01	0.184D+00	0.228D+00
2^{-24}	0.774D+00	0.382D+00	0.189D+00	0.882D−01	0.971D−01	0.191D+00
2^{-25}	0.773D+00	0.381D+00	0.188D+00	0.946D−01	0.597D−01	0.122D+00
2^{-26}	0.773D+00	0.381D+00	0.186D+00	0.912D−01	0.519D−01	0.698D−01
E^N	0.775D+00	0.475D+00	0.385D+00	0.346D+00	0.315D+00	0.228D+00

In Table IV we show the computed v-uniform orders of convergence R^N, the computed v-uniform order of convergence R^*, the quantities $C_{R^*}^N$ and the computed v-uniform maximum error bounds, $C_{R^*}^* N^{-R^*}$. These are determined as follows. From the first row of Table IV we see that the orders R^N and that the minimum of these values gives $R^* = 0.98$. With this information, and the values of D^N in Table II, we find the computed error constants $C_{0.98}^N$ and hence $C_{0.98}^*$, which gives the second row of Table IV. The third row, i.e. $C_{0.98}^* N^{-0.98}$, is obtained immediately from the second, and the fourth row, i.e. E^N, is simply part of the last row of Table I.

If the computed v-uniform error bounds are indeed error bounds, then it is to be expected that they should be larger than the computed v-uniform errors. Inspection of the last two rows of Table IV shows that this is the case. We conclude from these tables that the method (11), (12),

Copyright © 2006 John Wiley & Sons, Ltd.

DOI: 10.1002/fld

Table VII. Two mesh differences D_v^N for various values of v and N on a *uniform* mesh.

	Number of intervals N				
v	32	64	128	256	512
2^{-1}	0.562D−01	0.294D−01	0.150D−01	0.757D−02	0.380D−02
2^{-2}	0.130D+00	0.686D−01	0.352D−01	0.178D−01	0.896D−02
2^{-3}	0.231D+00	0.121D+00	0.620D−01	0.314D−01	0.158D−01
2^{-4}	0.292D+00	0.151D+00	0.770D−01	0.389D−01	0.195D−01
2^{-5}	0.272D+00	0.138D+00	0.698D−01	0.350D−01	0.176D−01
2^{-6}	0.232D+00	0.117D+00	0.590D−01	0.295D−01	0.148D−01
2^{-7}	0.227D+00	0.114D+00	0.575D−01	0.289D−01	0.145D−01
2^{-8}	0.227D+00	0.113D+00	0.568D−01	0.285D−01	0.143D−01
2^{-9}	0.229D+00	0.114D+00	0.567D−01	0.283D−01	0.142D−01
2^{-10}	0.234D+00	0.115D+00	0.570D−01	0.308D−01	0.207D−01
2^{-11}	0.247D+00	0.119D+00	0.602D−01	0.486D−01	0.251D−01
2^{-12}	0.271D+00	0.130D+00	0.976D−01	0.494D−01	0.246D−01
2^{-13}	0.322D+00	0.195D+00	0.982D−01	0.492D−01	0.247D−01
2^{-14}	0.389D+00	0.196D+00	0.982D−01	0.492D−01	0.247D−01
2^{-15}	0.393D+00	0.265D+00	0.106D+00	0.492D−01	0.247D−01
2^{-16}	0.393D+00	0.264D+00	0.189D+00	0.555D−01	0.247D−01
2^{-17}	0.393D+00	0.216D+00	0.243D+00	0.112D+00	0.283D−01
2^{-18}	0.393D+00	0.196D+00	0.225D+00	0.190D+00	0.561D−01
2^{-19}	0.393D+00	0.196D+00	0.167D+00	0.234D+00	0.116D+00
2^{-20}	0.393D+00	0.196D+00	0.120D+00	0.205D+00	0.191D+00
2^{-21}	0.393D+00	0.196D+00	0.985D−01	0.141D+00	0.230D+00
2^{-22}	0.395D+00	0.196D+00	0.982D−01	0.935D−01	0.196D+00
2^{-23}	0.394D+00	0.200D+00	0.987D−01	0.660D−01	0.129D+00
2^{-24}	0.393D+00	0.198D+00	0.105D+00	0.572D−01	0.776D−01
2^{-25}	0.393D+00	0.197D+00	0.102D+00	0.611D−01	0.490D−01
2^{-26}	0.393D+00	0.197D+00	0.100D+00	0.552D−01	0.416D−01
D^N	0.395D+00	0.265D+00	0.243D+00	0.234D+00	0.230D+00

satisfying (14), is robust with respect to the singular perturbation parameter v and that its v-uniform order of convergence is nearly 1.

We remark that, at first sight it may be tempting to determine computed v-uniform orders of convergence from Table III by taking the minimum value in each column and then taking the minimum of these minimum values as the final computed v-uniform order of convergence. That this gives an excessively pessimistic result is borne out by, and is one of the main results of, the experimental error analysis given in Table IV.

We now consider Table V which indicates the number of iterations required to achieve the specified tolerance 10^{-3} in (14). We define

$$I^N = \max_v I_v^N$$

where I_v^N is the number of iterations required to achieve this tolerance.

Copyright © 2006 John Wiley & Sons, Ltd.

DOI: 10.1002/fld

Table VIII. Orders of convergence R_v^N for various values of v and N on a *uniform* mesh.

	Number of intervals N			
v	32	64	128	256
2^{-0}	0.96	0.98	0.99	0.99
2^{-1}	0.94	0.97	0.99	0.99
2^{-2}	0.93	0.96	0.98	0.99
2^{-3}	0.93	0.97	0.98	0.99
2^{-4}	0.95	0.97	0.99	0.99
2^{-5}	0.97	0.99	0.99	1.00
2^{-6}	0.99	0.99	1.00	1.00
2^{-7}	0.99	0.99	0.99	1.00
2^{-8}	1.00	1.00	0.99	1.00
2^{-9}	1.01	1.00	1.00	1.00
2^{-10}	1.02	1.02	0.89	0.58
2^{-11}	1.05	0.99	0.31	0.95
2^{-12}	1.06	0.42	0.98	1.00
2^{-13}	0.73	0.99	1.00	0.99
2^{-14}	0.98	1.00	1.00	0.99
2^{-15}	0.57	1.32	1.11	0.99
2^{-16}	0.57	0.48	1.77	1.17
2^{-17}	0.87	−0.17	1.12	1.99
2^{-18}	1.00	−0.19	0.24	1.76
2^{-19}	1.00	0.24	−0.49	1.02
2^{-20}	1.00	0.71	−0.77	0.10
2^{-21}	1.00	1.00	−0.52	−0.71
2^{-22}	1.01	1.00	0.07	****
2^{-23}	0.97	1.02	0.58	−0.96
2^{-24}	0.99	0.92	0.88	−0.44
2^{-25}	0.99	0.95	0.74	0.32
2^{-26}	1.00	0.98	0.86	0.41
R^N	0.58	0.13	0.05	0.03

We see that, for each fixed value of v, as N increases the number of iterations reduces, as expected. More importantly, it is apparent from this table that, as v reduces, for each fixed N, the number of iterations required decreases and stabilizes. It is this result that confirms that the numerical approximations generated by this method converge to the solution v-uniformly and independently of the period.

With standard numerical methods (i.e. methods that do not use a fitted piecewise uniform mesh), as v decreases and the layer gets thinner, extremely fine meshes are required to capture the activity within the layer. This is not an acceptable situation. To verify this claim we show in Figure 2 the solution of the problem on a uniform mesh with $N = 32$ and $v = 2^{-5}$ and $v = 2^{-10}$. We see from this figure that, for $v = 2^{-10}$, the activity inside the layer region close to the wall is 'not smooth' in comparison to the situation in Figure 1. This means that the uniform mesh

Copyright © 2006 John Wiley & Sons, Ltd.

DOI: 10.1002/fld

Table IX. Errors E_v^N for various values of v and N on a *uniform* mesh, with the finest mesh $N = 2048$ computed on a piecewise uniform mesh.

	Number of intervals N					
v	32	64	128	256	512	1024
2^{-0}	0.453D−01	0.228D−01	0.112D−01	0.525D−02	0.226D−02	0.754D−03
2^{-1}	0.113D+00	0.575D−01	0.282D−01	0.133D−01	0.571D−02	0.191D−02
2^{-2}	0.264D+00	0.135D+00	0.664D−01	0.313D−01	0.135D−01	0.449D−02
2^{-3}	0.468D+00	0.238D+00	0.117D+00	0.551D−01	0.237D−01	0.792D−02
2^{-4}	0.587D+00	0.296D+00	0.145D+00	0.682D−01	0.293D−01	0.979D−02
2^{-5}	0.540D+00	0.269D+00	0.131D+00	0.614D−01	0.263D−01	0.878D−02
2^{-6}	0.458D+00	0.227D+00	0.110D+00	0.516D−01	0.221D−01	0.738D−02
2^{-7}	0.449D+00	0.222D+00	0.108D+00	0.506D−01	0.217D−01	0.723D−02
2^{-8}	0.446D+00	0.220D+00	0.107D+00	0.499D−01	0.214D−01	0.724D−02
2^{-9}	0.447D+00	0.219D+00	0.106D+00	0.495D−01	0.212D−01	0.719D−02
2^{-10}	0.457D+00	0.223D+00	0.108D+00	0.516D−01	0.322D−01	0.115D−01
2^{-11}	0.473D+00	0.237D+00	0.142D+00	0.862D−01	0.377D−01	0.126D−01
2^{-12}	0.508D+00	0.300D+00	0.184D+00	0.863D−01	0.370D−01	0.124D−01
2^{-13}	0.609D+00	0.379D+00	0.184D+00	0.862D−01	0.371D−01	0.124D−01
2^{-14}	0.769D+00	0.380D+00	0.184D+00	0.862D−01	0.371D−01	0.124D−01
2^{-15}	0.773D+00	0.425D+00	0.184D+00	0.862D−01	0.371D−01	0.124D−01
2^{-16}	0.773D+00	0.475D+00	0.265D+00	0.862D−01	0.371D−01	0.124D−01
2^{-17}	0.773D+00	0.402D+00	0.373D+00	0.149D+00	0.388D−01	0.124D−01
2^{-18}	0.773D+00	0.380D+00	0.387D+00	0.264D+00	0.750D−01	0.194D−01
2^{-19}	0.773D+00	0.380D+00	0.295D+00	0.353D+00	0.156D+00	0.406D−01
2^{-20}	0.773D+00	0.380D+00	0.186D+00	0.344D+00	0.267D+00	0.782D−01
2^{-21}	0.773D+00	0.380D+00	0.184D+00	0.239D+00	0.345D+00	0.160D+00
2^{-22}	0.775D+00	0.380D+00	0.184D+00	0.129D+00	0.323D+00	0.268D+00
2^{-23}	0.774D+00	0.384D+00	0.184D+00	0.922D−01	0.211D+00	0.341D+00
2^{-24}	0.774D+00	0.382D+00	0.189D+00	0.882D−01	0.968D−01	0.313D+00
2^{-25}	0.773D+00	0.381D+00	0.188D+00	0.947D−01	0.579D−01	0.196D+00
2^{-26}	0.773D+00	0.381D+00	0.186D+00	0.909D−01	0.526D−01	0.804D−01
E^N	0.775D+00	0.475D+00	0.387D+00	0.353D+00	0.345D+00	0.341D+00

is not sufficiently fine to capture this in-layer activity in this case. To emphasize experimentally the shortcomings of a uniform mesh to analyse the numerical solution of this problem we now recompute, using a uniform mesh, but to fully illustrate this behaviour we consider the complete tables, all results are given in Tables VI–IX. Table VI shows the errors with respect to the finest mesh corresponding to $N = 2048$. In addition, Table VII and VIII give the errors and the corresponding orders of convergence with respect to the two mesh differences. The results in these tables display erratic behaviour of the errors as the singular perturbation parameter decreases. This once again signifies the inefficiency of a uniform mesh for a singularly perturbed problem.

We further consider the numerical results computed in Table IX, this table shows a different approach to computing the errors. We still solve the problem on a uniform mesh but the finest mesh, for the reference solution, is computed on a piecewise uniform mesh. Once again this table

Copyright © 2006 John Wiley & Sons, Ltd.

DOI: 10.1002/fld

confirms the non-uniform behaviour seen when a uniform mesh is employed and the results are not parameter robust.

3. SUMMARY AND DISCUSSION OF RESULTS

For the periodic problems (1)–(6), we have constructed a monotone difference approximation. We have solved the problem on a special piecewise uniform mesh, which is defined using the asymptotic behaviour of the solution. With the aid of computational experiments, we have demonstrated that constructed numerical method gives numerical solutions for which the errors are independent of the viscosity v. We have contrasted the results with the results associated with employing a uniform mesh for the problem and clearly the results support our constructed numerical method on a non-uniform mesh. In addition, we have demonstrated experimentally that the number of iterations required to solve the discrete problem with this algorithm is independent of v. In addition, it is worth noting that one can easily attain the same results for increasing n while the viscosity is kept constant. The increasing value of n would correspond to an increasing pumping frequency. One practical application that lends itself to such a case is in the area of blood flow models. Furthermore, we also note that the parameter-robust behaviour attained is for a periodic problem.

ACKNOWLEDGEMENTS

This work was supported in part by the Enterprise Ireland Research Grant SC-2000-070, by the Russian Foundation for Basic Research Grant No. 04-01-00578 and by the Department of Mathematics and Statistics, University of Limerick.

REFERENCES

1. Shishkin GI. A difference scheme on a non-uniform mesh for a differential equation with a small parameter in the highest derivative. *U.S.S.R. Computational Mathematics and Mathematical Physics* 1983; **23**:59–66.
2. Hegarty AF, Miller JJH, O'Riordan E, Shishkin GI. Special meshes for finite difference approximations to an advection-diffusion equation with parabolic layers. *Journal of Computational Physics* 1995; **117**:47–54.
3. Miller JJH, O'Riordan E, Shishkin GI. *Fitted Numerical Methods for Singular Perturbation Problems*. World Scientific: London, 1996.
4. Farrell PA, Hegarty AF, Miller JJH, O'Riordan E, Shishkin GI. *Robust Computational Techniques for Boundary Layers*. Chapman & Hall/CRC Press: Boca Raton, FL, 2000.
5. Ansari AR, Hegarty AF, Shishkin GI. Parameter-uniform numerical methods for a laminar jet problem. *International Journal for Numerical Methods in Fluids* 2003; **43**(8):937–951.
6. Miller JJH, Musgrave AP, Shishkin GI. A Reynolds uniform numerical method for the Prandtl solution and its derivatives for stagnation line flow. *International Journal for Numerical Methods in Fluids* 2003; **43**(8):881–894.
7. Butler JS, Miller JJH, Shishkin GI. A Reynolds-uniform numerical method for Prandtl's boundary layer problem for flow past a wedge. *International Journal for Numerical Methods in Fluids* 2003; **43**(8):903–913.
8. Schlichting H. *Boundary-Layer Theory* (7th edn). McGraw Hill: New York, 1979.
9. Warsi ZUA. *Fluid Dynamics: Theoretical and Computational Approaches*. CRC Press: Boca Raton, 1993.
10. Prandtl L, Tietjens OG. *Applied Hydro- and Aeromechanics*. Dover Publications: New York, 1957.
11. Shishkin GI. Grid Approximations of singularly perturbed elliptic and parabolic equations. Ural Branch of Russian Academic Science, Ekaterinburg 1992 (in Russian).
12. Roos H-G, Stynes M, Tobiska L. *Numerical Methods for Singularly Perturbed Differential Equations. Convection–Diffusion and Flow Problems*. Springer: Berlin, 1996.

Copyright © 2006 John Wiley & Sons, Ltd.

DOI: 10.1002/fld